

OAK RIDGE
NATIONAL LABORATORY

MANAGED BY UT-BATTELLE
FOR THE DEPARTMENT OF ENERGY

ORNL/TM-2000/263

Cavitation in a Mercury Target

C. D. West



ORNL-27 (4-00)

DOCUMENT AVAILABILITY

Reports produced after January 1, 1996, are generally available free via the U.S. Department of Energy (DOE) Information Bridge.

Web site <http://www.osti.gov/bridge>

Reports produced before January 1, 1996, may be purchased by members of the public from the following source.

National Technical Information Service
5285 Port Royal Road
Springfield, VA 22161
Telephone 703-605-6000 (1-800-553-6847)
TDD 703-487-4639
Fax 703-605-6900
E-mail info@ntis.fedworld.gov
Web site <http://www.ntis.gov/support/ordernowabout.htm>

Reports are available to DOE employees, DOE contractors, Energy Technology Data Exchange (ETDE) representatives, and International Nuclear Information System (INIS) representatives from the following source.

Office of Scientific and Technical Information
P.O. Box 62
Oak Ridge, TN 37831
Telephone 865-576-8401
Fax 865-576-5728
E-mail reports@adonis.osti.gov
Web site <http://www.osti.gov/contact.html>

This report was prepared as an account of work sponsored by an agency of the United States Government. Neither the United States Government nor any agency thereof, nor any of their employees, makes any warranty, express or implied, or assumes any legal liability or responsibility for the accuracy, completeness, or usefulness of any information, apparatus, product, or process disclosed, or represents that its use would not infringe privately owned rights. Reference herein to any specific commercial product, process, or service by trade name, trademark, manufacturer, or otherwise, does not necessarily constitute or imply its endorsement, recommendation, or favoring by the United States Government or any agency thereof. The views and opinions of authors expressed herein do not necessarily state or reflect those of the United States Government or any agency thereof.

CAVITATION IN A MERCURY TARGET

C. D. West

Date Published: September 2000

Prepared by
OAK RIDGE NATIONAL LABORATORY
Oak Ridge, Tennessee 37831-6285
managed by
UT-BATTELLE, LLC
for the
U.S. DEPARTMENT OF ENERGY
under contract DE-AC05-00OR22725

CONTENTS

| | Page |
|---|-------------|
| ABSTRACT | 1 |
| 1. INTRODUCTION | 1 |
| 2. THE NUCLEATION PROCESS | 2 |
| 3. THRESHOLD FOR MACROSCOPIC BUBBLE FORMATION | 4 |
| 4. AVAILABLE ENERGY | 4 |
| 5. CALCULATION OF THRESHOLDS | 9 |
| 6. RESULTS | 9 |
| 7. EXPERIMENTAL DATA | 11 |
| 8. SUMMARY | 12 |
| Appendix A: DOMINANCE OF KINETIC TERMS | 13 |
| Appendix B: PROPERTIES OF MERCURY FOR SNS TARGET CAVITATION CALCULATIONS | 15 |
| REFERENCES | 17 |

LIST OF FIGURES

| Figure | | Page |
|--------|--|------|
| 1 | Enthalpies of isopentane | 3 |
| 2 | Range of ^{202}Hg in natural mercury (second-order polynomial fit) | 5 |
| 3 | Bubble nucleation threshold for initial energies up to 20 MeV | 10 |
| 4 | Bubble nucleation threshold for initial energies below 1 MeV | 10 |

LIST OF TABLES

| Table | | Page |
|-------|--|------|
| 1 | Some bubble formation experiments with isopentane | 3 |
| 2 | Range and dE/dx for ^{202}Hg in natural mercury | 5 |
| 3 | Values of R_0 calculated from the quintic equation and from the approximate formula | 8 |
| 4 | Radius of nucleation center, R_0 | 9 |
| 5 | Recoil energies and calculated threshold | 11 |

CAVITATION IN A MERCURY TARGET

C. D. West

ABSTRACT

Recent theoretical work on the formation of bubble nucleation centers by energetic particles leads to some reasonably credible calculations of the maximum negative pressure that might be sustained without bubble formation in the mercury target of the Spallation Neutron Source.

1. INTRODUCTION

In a sufficiently superheated liquid, the energy deposited by an energetic particle can cause local boiling that, after a short time, leads to a bubble of visible size. This effect was sought and observed in 1952 by Donald Glaser, during the course of his well-thought-out and persistent search for a new device that could reveal the tracks of high-energy particles. For a wonderful description of the desired properties of the detector and the thought process and experiments that led him to developing the bubble chamber and subsequently receiving a Nobel Prize for his research, see Glaser (1994).

The idea of bubble nucleation by the local formation of vapor evolved gradually; initially, the mechanism was imagined to be an electrostatic one, like the formation of droplets in the Wilson Cloud Chamber (which was already well known). In 1957, an influential paper written by Frederick Seitz—the first paper in the first edition of the first volume of a new journal, *Physics of Fluids*—quantified the local boiling theory, equating the energy expected to be deposited by the particle to the latent heat of vaporization and other smaller energy terms involved in the formation of the bubble (Seitz, 1957). This theory was beautifully confirmed by experimental measurements carried out by graduate student Georg Riepe (Riepe and Hahn, 1961). The experiments involved measuring the degree of superheating necessary to form bubbles around the tracks of ^{210}Po , ^{212}Po , and ^{212}Bi alpha recoils in propane and Freon 12. The liquid temperature was in the typical operating region of a bubble chamber—approximately two-thirds of the way between the normal boiling point and the critical temperature—and the liquid was initially held at its saturation pressure, so no boiling occurred. The pressure reduction needed to form bubbles from the alpha decay of polonium, or thorium C and thorium C', dissolved in the liquid was then measured. The calculated energy balance of bubble nucleation and the energy available from the decay matched the prediction of Seitz's theory within a few percent, a great achievement.

When similar experiments were later carried out with cold liquids, below their normal boiling points, the liquids had to be placed under negative pressure (i.e., tensile stress) for macroscopic bubbles to be formed by alpha decay recoil particles (Hahn, 1961). The calculated energy balance typically differed by an order of magnitude from calculations based on Seitz's theory of the positive-pressure bubble chamber (Hahn and Peacock, 1963). It was soon recognized (West, 1967) that Seitz's basic physical model of local heating could also be applied to this situation, but that a different algebraic formulation of the model was appropriate for liquids under large negative pressures. However, although a fundamental reason for the discrepancy was thus identified, quantitative agreement between the calculated and measured pressure threshold

for bubble formation, although improved, was still very poor compared with the agreement achieved by Riepe and Hahn's bubble chamber results.

More recently, a further development of the theory has led to much improved agreement (West, 1998), and that new model is applied in this report to calculate the minimum negative pressure that might be required to nucleate bubbles by recoiling mercury nuclei or heavy decay products of mercury in the target of the Spallation Neutron Source (SNS), planned at Oak Ridge.

2. THE NUCLEATION PROCESS

An energetic particle that is slowing down gives up its kinetic energy to atoms of the medium; that is, it heats the medium locally along its track. The heating can cause local vaporization, thus forming a small bubble. If that bubble is large enough, the pressure of vapor inside can overcome the surface tension forces tending to collapse it, and the bubble will grow indefinitely. A smaller bubble will soon collapse and disappear as surface tension raises the internal pressure enough to recondense the vapor. The growth, if it is to occur at all, must take place in a very short time, because the small amount of heat involved within a very small volume is soon dissipated, by conduction, into the surrounding liquid.

Two energetic conditions must be satisfied to turn a small heated volume of liquid into vapor: (1) there must be enough energy to provide the enthalpy of evaporation (this is the largest energy term in Seitz's bubble chamber theory), and (2) the liquid must be hot enough that the probability of spontaneous nucleation of boiling within that volume is high.

The second condition may require some further explanation. It has long been known that although most pure liquids have a well-defined boiling point, a clean sample in a clean container can often be raised to a much higher temperature before boiling erupts; in fact, the classic advice given to physicists (e.g., Chute, 1896) is to measure boiling points by placing a thermometer in the vapor above the boiling liquid rather than in the liquid itself. A simple criterion for spontaneous nucleation to occur, used by West (1998), is that the small heated volume be raised to the critical point, in which case it can certainly no longer remain liquid.

It turns out that in hot liquids, such as in a bubble chamber, the enthalpy difference, H_{ca} , between the subcooled ambient condition and the critical point is less than the enthalpy of evaporation, H_{vap} , so that if the energy deposition from a particle is sufficient to evaporate enough liquid to form a bubble of the critical size (Seitz's criterion), it is also enough to ensure homogeneous nucleation. In a cold liquid, the opposite is true, and in order for a particle to have a high probability of forming a macroscopic bubble, it must deposit more energy than the Seitz criterion alone would require. Remember that Seitz explicitly and appropriately applied his theory to the former situation only. Figure 1 compares the two enthalpy terms for a particular liquid, isopentane, that has been used both in bubble chambers and in cavitation experiments (Table 1). It is unfortunate that no measurements have been reported on the temperature dependence of the threshold for negative- and positive-pressure bubble nucleation by the same source of particles, such as neutrons or a dissolved alpha emitter, in the same liquid—an experiment that begs to be done.

Table 1. Some bubble formation experiments with isopentane

| Experiment or property | Radiation | Temperature (°C) | References |
|---|-------------------------|------------------|------------------------|
| Spinner experiment | ^{210}Po decay | 20 | Hahn, 1961 |
| Ultrasonic cavitation | Fast neutrons | ~21? | Lieberman, 1959 |
| Ultrasonic cavitation | Fast neutrons | ~25 | Hughes, 1960 |
| Normal boiling point | | 28 | Yaws, 1996 |
| Negative-pressure bubble chamber | Minimum ionization | 120 | Pless and Plano, 1956 |
| Superheat limit at atmospheric pressure | Cosmic? | 139 | Blander and Katz, 1975 |
| Normal bubble chamber | Minimum ionization | 157 | Glaser and Rahm, 1955 |
| Critical temperature | | 187 | Yaws, 1996 |

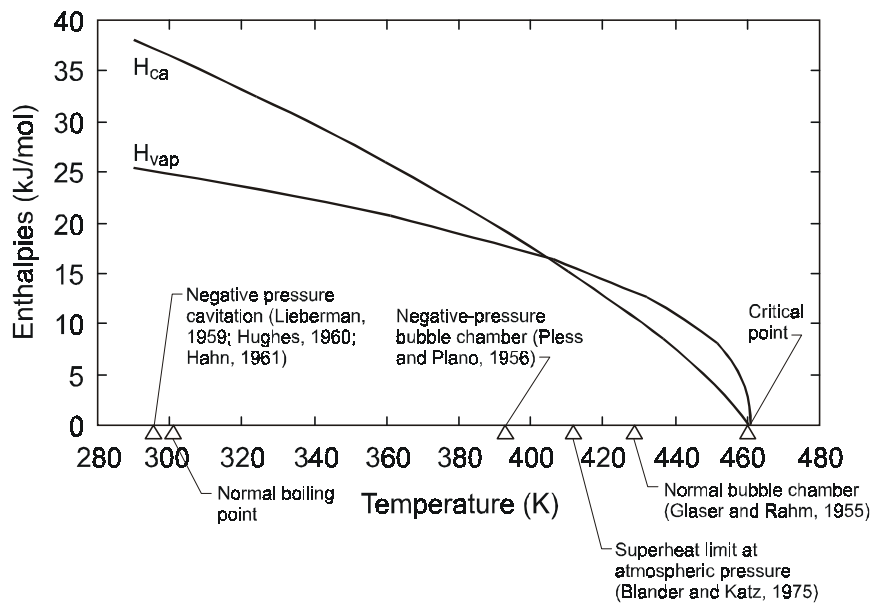


Fig. 1. Enthalpies of isopentane.

3. THRESHOLD FOR MACROSCOPIC BUBBLE FORMATION

Estimation of the minimum negative pressure that will form a macroscopic cavitation bubble from a certain amount of energy, E_{av} , provided by an energetic particle is rather complicated, even in the particular case where the linear rate of energy deposition, dE/dx , is independent of the energy (West, 1998). Besides the enthalpy difference, H_{ca} , the threshold depends on the surface tension and density of the liquid, its density and pressure at the critical point, its viscosity, its thermal diffusivity, and the value of dE/dx or the initial energy of the particle.

Fortunately, the problem is greatly simplified if the energy requirements of the initial bubble formation are dominated by kinetic terms, that is, by the viscosity and/or the amount of kinetic energy that must be imparted to the liquid around the growing bubble if it is to reach the critical size before its heat content is lost by conduction. It turns out that this is true for mercury, as shown in Appendix A. In such a case, the minimum negative pressure P_{neg} (threshold) that will lead to a bubble of macroscopic size is given by a simple equation, Eq. (63) in West (1998):

$$P_{neg} \text{ (threshold)} = 2\sigma \sqrt[3]{\frac{4\pi\rho_{crit}H_{ca}}{3E_{av}}}, \quad (1)$$

where

- σ = the surface tension,
- ρ_{crit} = the density at the critical point,
- H_{ca} = the enthalpy difference between the initial condition and the critical point, and
- E_{av} = the available energy (described in Sect. 4).

Liquid enthalpy values do not appear to be available for negative-pressure conditions, but liquid enthalpy is not very dependent on pressure and for convenience is here evaluated at the initial temperature of the liquid and at a pressure 1% above the corresponding saturation pressure (to ensure that the evaluation is made under conditions where the substance is a liquid, not a vapor). The mercury properties needed for the calculations were taken from the Yaws data base (Yaws, 1996) and are listed in Appendix B.

4. AVAILABLE ENERGY

Peter Fu kindly provided calculated values for the range and dE/dx of ^{202}Hg in a medium of natural mercury (Fu, 1999). Some of his data, calculated from a version of the SPAR code that he modified to work with higher-atomic-number particles, are listed in Table 2. The upper energy limit shown in the table is approximately 20 MeV, which would be the maximum energy that could be given to an elastically recoiling mercury atom by a 1-GeV proton—the proton energy in the SNS.

Examination of Table 2 shows that in this range of energies, the linear rate of energy deposition, dE/dx , is highest at the beginning of the particle's track. Therefore, the energy available, E_{av} , over any distance less than the range is greatest at the beginning of the track.

Because dE/dx is energy dependent, the range is not proportional to the initial energy, but Fig. 2 (prepared with TK Solver) shows that a second-order polynomial relationship fits the data well.

Table 2. Range and dE/dx for ^{202}Hg in natural mercury

| Initial energy (MeV) | Range ($\times 10^{-5}$ cm) | Initial dE/dx ($\times 10^5$ MeV/cm) |
|-------------------------|---------------------------------|--|
| 21.15 | 17.711 | 1.461 |
| 19.41 | 16.498 | 1.423 |
| 17.81 | 15.369 | 1.388 |
| 14.99 | 13.289 | 1.325 |
| 10.63 | 9.873 | 1.226 |
| 5.34 | 5.346 | 1.111 |
| 4.90 | 4.949 | 1.104 |
| 2.07 | 2.311 | 1.034 |
| 1.04 | 1.290 | 0.978 |
| 0.956 | 1.202 | 0.970 |
| 0.738 | 0.974 | 0.944 |
| 0.523 | 0.743 | 0.904 |
| 0.480 | 0.694 | 0.894 |
| 0.203 | 0.365 | 0.772 |
| 0.102 | 0.225 | 0.663 |
| 0.051 | 0.142 | 0.552 |

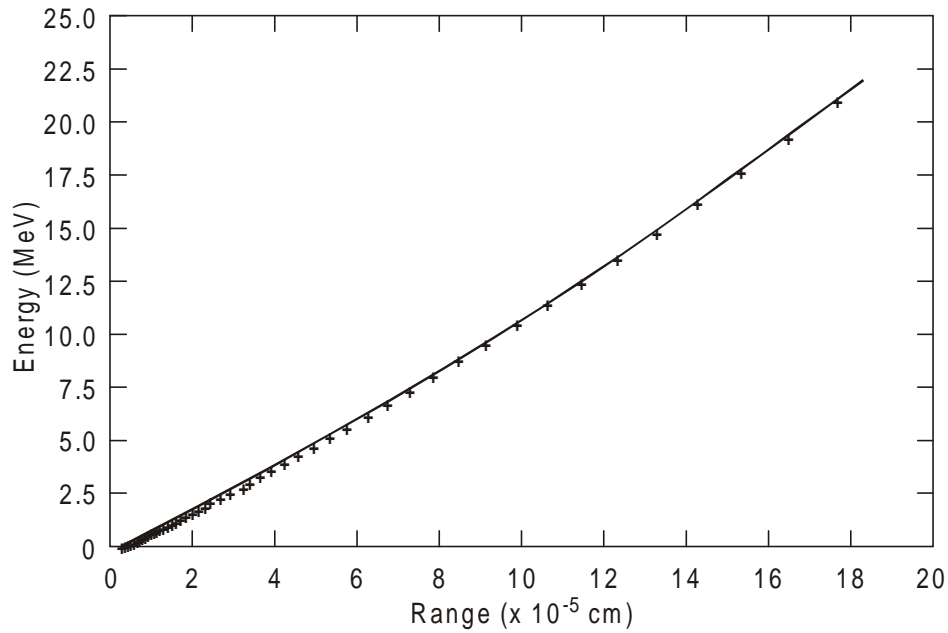


Fig. 2. Range of ^{202}Hg in natural mercury (second-order polynomial fit).

Changing to S.I. units for convenience in the calculations to follow, the equation of the fitted curve, with range R measured metres and energy in joules, is

$$R(E) \approx r_1 + r_2 E + r_3 E^2 , \quad (2)$$

where

$$\begin{aligned} r_1 &= 2.091 \times 10^{-8} \text{ m}, \\ r_2 &= 6.275 \times 10^5 \text{ m/J}, \text{ and} \\ r_3 &= -3.371 \times 10^{16} \text{ m/J}^2. \end{aligned}$$

The enthalpy that must be added to form a sphere of fluid with radius R_o at the critical point is

$$E = \frac{4}{3} \pi R_o^3 \rho_{\text{crit}} H_{\text{ca}} ,$$

and the largest possible nucleation center is formed when

$$\frac{4}{3} \pi R_o^3 \rho_{\text{crit}} H_{\text{ca}} = E_{\text{av}} , \quad (3)$$

where E_{av} is the energy deposited, by the recoil, in a distance of $2R_o$ [see Sect. 8.3 of West (1998)].

If the recoil track is very long, the largest nucleation center will be formed in the first part of the track where dE/dx is highest; if the track is short enough, it will be formed using the whole recoil energy.

In the former case, one can calculate the energy E_{av} deposited in a distance $2R_o$ from the beginning of the track by writing

$$\text{Range}(E_{\text{initial}}) - \text{Range}(E_{\text{initial}} - E_{\text{av}}) = 2R_o .$$

Now substitute the range-vs-energy relationship of Eq. (2),

$$(r_1 + r_2 E_{\text{initial}} + r_3 E_{\text{initial}}^2) - [r_1 + r_2 (E_{\text{initial}} - E_{\text{av}}) + r_3 (E_{\text{initial}} - E_{\text{av}})^2] = R_o ,$$

or, rearranging and simplifying,

$$E_{\text{av}}^2 - (2E_{\text{initial}} + r_2/r_3) E_{\text{av}} + 2R_o/r_3 = 0 . \quad (4)$$

Now simplify the appearance of Eq. (3) by writing

$$H = \frac{4}{3} \pi \rho_{\text{crit}} H_{\text{ca}} .$$

The variable H is actually the enthalpy per unit volume needed to raise the liquid to the critical point multiplied by the constant $4\pi/3$. Equation (3) now reads

$$E_{\text{av}} = HR_0^3 \quad , \quad (5)$$

and substituting that relationship into Eq. (4) yields

$$H^2 R_0^6 - (2E_{\text{initial}} + r_2/r_3) HR_0^3 + 2R_0/r_3 = 0 \quad ,$$

or dividing by $H^2 R_0^6$,

$$R_0^5 - \frac{2E_{\text{initial}} + r_2/r_3}{H} R_0^2 + \frac{2/r_3}{H^2} = 0 \quad . \quad (6a)$$

The roots of this quintic equation can easily be found numerically, for example by using the BISECT program in the TK Solver library. However, in the range of values for E_{initial} of interest in this report ($E_{\text{initial}} < 20$ MeV), it turns out that the fifth-order term is negligible.

For example, if $E_{\text{initial}} = 20$ MeV,

$$E_{\text{initial}} = 20 \text{ MeV} = 3.204 \times 10^{-12} \text{ J} \quad ,$$

$$r_2/r_3 = 6.275 \times 10^5 / (-3.371 \times 10^{16}) = -18.61 \times 10^{-12} \text{ J} \quad ,$$

$$H = (4\pi/3) \times 17.746 \times 10^3 \times 62.00 \times 10^3 = 4.608 \times 10^9 \text{ J/m}^3 \quad ,$$

and Eq. (6a) becomes

$$R_0^5 + 2.65 \times 10^{-21} R_0^2 - 2.79 \times 10^{-36} = 0 \quad .$$

The solution for R_0 obtained by ignoring the fifth-order term is

$$R_0 = \sqrt{\left(2.794 \times 10^{-36} / 2.65 \times 10^{-21}\right)} = 32.5 \text{ nm} \quad .$$

Then $R_0^5 \sim 3.6 \times 10^{-38}$, which is two orders of magnitude less than the constant term of 2.79×10^{-36} . Therefore Eq. (6a), for this liquid in this range of particle energies, can be approximated by

$$R_0 \approx \sqrt{\frac{1}{H(r_3 E_{\text{initial}} + r_2/2)}} \quad . \quad (6b)$$

To verify this, Table 3 compares values of R_0 computed from Eqs. (6a) and (6b) over a range of initial energies from 0.1 to 20 MeV. The values from Eq. (6b) are all within 1% of the

Table 3. Values of R_o calculated from the quintic equation and from the approximate formula

| Initial energy (MeV) | R_o from Eq. (6a) (nm) | R_o from Eq. (6b) (nm) |
|-------------------------|-----------------------------|-----------------------------|
| 0.1 | 26.264 | 26.322 |
| 0.2 | 26.286 | 26.345 |
| 0.4 | 26.331 | 26.391 |
| 0.8 | 26.422 | 26.483 |
| 1.0 | 26.467 | 26.529 |
| 2.0 | 26.700 | 26.765 |
| 4.0 | 27.182 | 27.255 |
| 8.0 | 28.231 | 28.322 |
| 10.0 | 28.802 | 28.905 |
| 20.0 | 32.274 | 32.478 |

solution from Eq. (6a), and the rest of these calculations will therefore use the approximate, but much simpler, Eq. (6b).

The largest nucleation center that could possibly be formed, if all of the initial recoil energy were used, would have a radius R_o such that [see Eq. (3)]

$$E_{\text{initial}} = \frac{4}{3} \pi R_o^3 \rho_{\text{crit}} H_{\text{ca}} .$$

Substituting $H = (4\pi/3) \rho_{\text{crit}} H_{\text{ca}}$ and rearranging yields

$$R_o = \sqrt[3]{\frac{E_{\text{initial}}}{H}} . \quad (7)$$

However, if the total range of a recoil with energy E_{initial} is greater than $2R_o$, only that part of the energy deposited within a distance $2R_o$ would be available to the nucleation center, and Eq. (7) would apply. A convenient way of expressing this, particularly if TK Solver is used to evaluate the equations, based on the approximate Eq. (6b), is

$$R_o = \text{MIN} \left[\sqrt[3]{\frac{E_{\text{initial}}}{H}} , \sqrt{\frac{1}{H(r_3 E_{\text{initial}} + r_2/2)}} \right] , \quad (8)$$

where, in the language of TK Solver, $\text{MIN}(X, Y)$ means the smaller of the two values X and Y .

Table 4 shows the two parenthetical components in Eq. (8) and the corresponding calculated value of R_o .

Table 4. Radius of nucleation center, R_o^a

| E_{initial} (MeV) | R_o (nm) | | |
|-------------------------------|--|-------------------|------------------|
| | Based on Eq. (7) (using all the recoil energy) | Based on Eq. (6b) | Based on Eq. (8) |
| 0.1 | 15.150 | 26.322 | 15.150 |
| 0.2 | 19.087 | 26.345 | 19.087 |
| 0.4 | 24.048 | 26.391 | 24.048 |
| 0.8 | 30.299 | 26.483 | 26.483 |
| 1.0 | 32.639 | 26.529 | 26.529 |
| 2.0 | 41.122 | 26.765 | 26.705 |
| 4.0 | 51.811 | 27.255 | 27.255 |
| 8.0 | 65.278 | 28.322 | 28.322 |
| 10.0 | 70.318 | 28.905 | 28.905 |
| 20.0 | 88.595 | 32.478 | 32.478 |

^aNote that for energies above about 0.5 MeV, the recoil track is longer than the nucleation center diameter, so only a fraction of the recoil energy is available to initiate a single bubble.

5. CALCULATION OF THRESHOLDS

Now that R_o has been calculated, E_{av} can be determined from the relationship $E_{\text{av}} = HR_o^3$, and then the minimum negative pressure for bubble formation can be obtained from Eq. (1). However, there is a more direct method.

If we substitute $E_{\text{av}} = HR_o^3$, from Eq. (5), directly into Eq. (1), remembering that $H = (4\pi/3)\rho_{\text{crit}}H_{\text{ca}}$, the result is

$$P_{\text{neg}} (\text{threshold}) = \frac{2\sigma}{R_o} . \quad (9)$$

Such simplicity may seem surprising, but it is a consequence of the basic nucleation mechanism: a bubble of radius r feels an inward force from surface tension that tends to collapse it. That force is equivalent to an inward pressure of $2\sigma/r$, and any outward pressure (either from vapor inside the bubble or from an external negative pressure) that is greater than $2\sigma/r$ will cause the bubble to grow, hence Eq. (9).

To calculate the thresholds, for mercury recoils with initial energies in the range 0.1–20 MeV, use Eq. (8) to evaluate R_o , and substitute that value in Eq. (9) to calculate the threshold.

6. RESULTS

Figures 3 and 4 show the negative-pressure threshold calculated as a function of the initial energy of the recoil. The sudden change in the slope, at an initial energy of ~0.5 MeV, represents

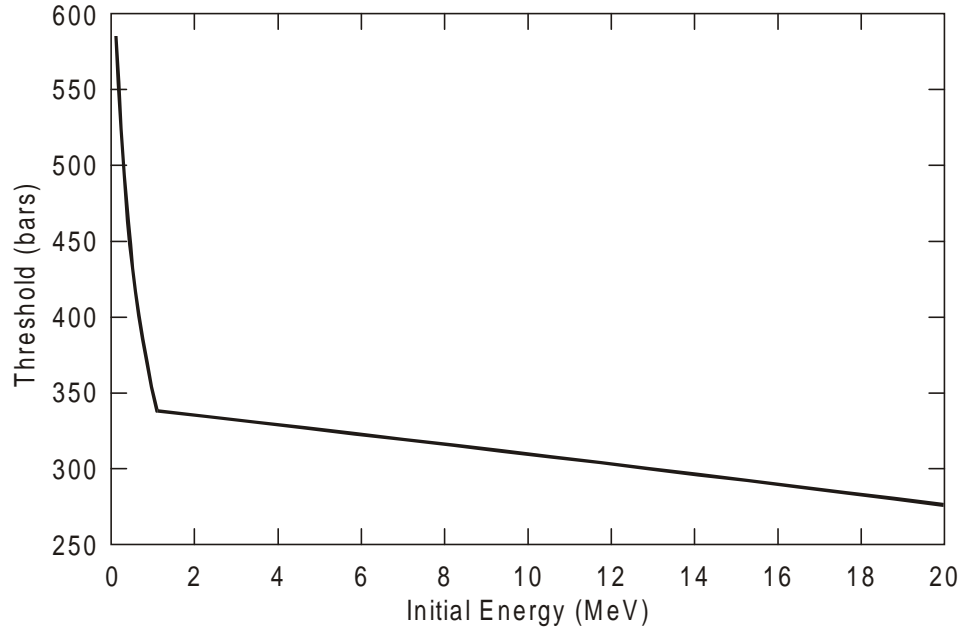


Fig. 3. Bubble nucleation threshold for initial energies up to 20 MeV.

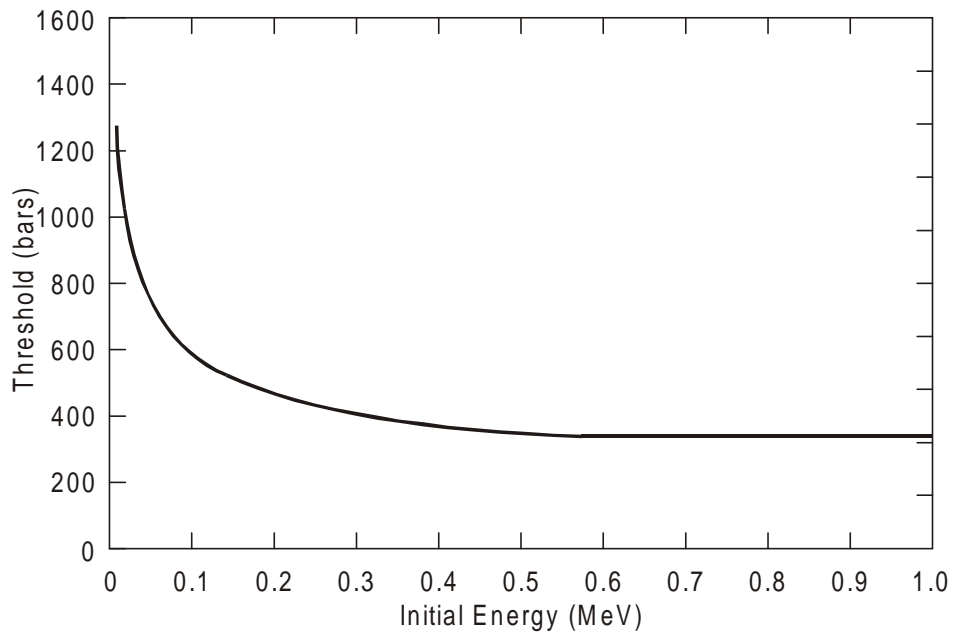


Fig. 4. Bubble nucleation threshold for initial energies below 1 MeV.

the point above which the range of the particle is so long that not all of its initial energy is deposited in a region small enough to form a single nucleation center. At higher energies, the threshold falls only slowly, as dE/dx gradually gets larger. In the range 0.5–20 MeV, the negative-pressure threshold is in the range 307 ± 30 bars. Below 0.5 MeV, it rises rapidly to over 700 bars at 50 keV.

I know of no published data concerning the radioactive or recoil particles expected to be found in the mercury target of the SNS. However, one can speculate on the outcome of various physical processes. As stated earlier, the maximum energy a mercury atom can receive from an incoming proton is 20 MeV, but the negative-pressure waves that might give rise to cavitation are generated by the reflection of positive-pressure waves created when the proton beam strikes and heats the target. Therefore, the mercury recoils will see no negative pressure to nucleate bubbles unless pressure waves continue to reverberate with a high amplitude until the next proton pulse, 15 ms later. This would require a high amplitude to be maintained following 200 or more reflections. The SNS Project is planning experiments to observe the reverberations, but such a long period of almost undiminished echoes seems unlikely.

Another possible source of recoils would be neutrons, or other particles, emitted by activated materials in the target mercury or its container. It would probably be conservative to assume that the maximum energy of such a particle would be 10 MeV, in which case the maximum energy it could give to a mercury nucleus, in a head-on elastic collision, would be ~ 200 keV. Or if the mercury itself were transmuted, without a great change of mass in the transmutation, the resulting isotope might recoil upon decay through alpha emission. If an alpha particle were emitted with an energy of, say, 5 MeV, then the maximum recoil energy of a particle of mass ~ 200 amu would be ~ 400 keV. The calculated negative-pressure thresholds for such events are shown in Table 5.

Table 5. Recoil energies and calculated threshold

| Mercury recoil energy (MeV) | Calculated threshold (bars) |
|--------------------------------|--------------------------------|
| 2.0 | 270 |
| 0.4 | 370 |
| 0.2 | 470 |

7. EXPERIMENTAL DATA

Briggs (1953) measured the cavitation threshold of mercury in Pyrex glass using his spinner method. Even taking extreme measures to clean the glass tube and to purify and degas the mercury, the maximum negative pressure sustained was 425 bars at 27°C (much lower than the 150°C expected in the SNS target), and in other circumstances the threshold was more typically less than 50 bars. Experiments by Taleyarkhan et al. (1998) and Moraga (1999) with mercury that had not been thoroughly degassed led to cavitation at less than 1 bar of negative pressure.

For comparison, calculations by Taleyarkhan and Kim (1998) of the negative-pressure pulse following reflection of the initial positive-pressure wave give a value of more than 200 bars in the bulk mercury and more than 600 bars near the target walls (if there was no significant cavitation). Experiments are planned to measure the amplitude of successive reflections. However, the experimental data mentioned in the previous paragraph seem to indicate that in a

practical mercury target, other mechanisms are likely to lead to a negative-pressure threshold for cavitation that is smaller (more easily reached) than the theoretical limit imposed by radiation-induced nucleation.

8. SUMMARY

One can make simple calculations of the ultimate negative pressure likely to be sustainable by the mercury of the SNS target. Radiation is likely to set an upper limit of ~400 bars, although dissolved or entrained gas will likely prevent such high tensile stresses from being reached in a practical target assembly.

Appendix A:
DOMINANCE OF KINETIC TERMS

Section 7.3 of West (1998) describes how to determine whether Eq. (1) of the present report is appropriate. In liquids where the dynamic terms (viscous losses and the kinetic energy given to the liquid around the rapidly growing bubble) are dominant, the bubble cannot grow fast enough to preserve the initial energy deposited by the nucleating particle. Instead, that energy is lost almost immediately by conduction so that the internal energy, and therefore pressure, inside the bubble soon becomes very small. To continue bubble growth beyond this stage, the negative pressure alone must be able to overcome the inward forces of surface tension, that is,

$$P_{\text{neg}} (\text{threshold}) \geq \frac{2\sigma}{R_o} , \quad (\text{A.1})$$

where σ is the surface tension and R_o the initial radius of the nucleation center. As indicated in Eq. (3) of this report,

$$R_o = 3 \sqrt{\frac{3E_{\text{av}}}{4\pi\rho_{\text{crit}}H_{\text{ca}}}} . \quad (\text{A.2})$$

The section referred to above (West, 1998) shows that the distinction between high and low dynamic-loss cases is determined by comparing the results predicted by Eqs. (44) and (50) of that report. With a slight change of nomenclature (substituting E_{av} for E_{recoil}), Eq. (50) is identical to Eq. (A.2) above.

Using the TK Solver routines developed for the work reported by West (1998), the results for mercury are calculated as follows:

| E_{av} (MeV) | P_{neg} (threshold) (bars) | |
|--------------------------|--|----------|
| | Eq. (44) | Eq. (50) |
| 20 | 299 | 101* |
| 2 | 22,976 | 218* |
| 0.2 | 2,230,447 | 470 |

In all cases Eq. (50) is by far the lower value, indicating that Eq. (50) or (A.2) is the appropriate one to use.

*These values are lower than those that appear in Table 5, which is seemingly similar. The energy listed in Table 5 is the total recoil energy, not all of which is available for bubble formation.

Appendix B:
PROPERTIES OF MERCURY FOR SNS TARGET
CAVITATION CALCULATIONS

| Property | Units | Value | Notes |
|---|---------------------|------------------------|--|
| Z_p | | 80 | Charge number of recoiling particle |
| T_{amb} | K | 423.15 | Initial temperature |
| Data obtained from Yaws database | | | |
| Mwt | g/mol | 200.59 | Molecular weight |
| Z_ℓ | | 80 | Charge number of medium |
| ρ_ℓ | kg/m ³ | 13,270 | Density of liquid |
| sigma | mN/m | 447.47 | Surface tension |
| C _{pliq} | J/mol·K | 27.54 | Specific heat |
| eta | mPa/s | 1.165 | Viscosity |
| k _{liq} | w/m·K | 10.05 | Thermal conductivity |
| P_{crit} | bars | 1608 | Critical pressure |
| T_{crit} | K | 1735 | Critical temperature |
| ρ_{crit} | kg/m ³ | 3559.7 | Density at critical point |
| H_{ca} | Btu/lb | 132.95 | Enthalpy difference, ambient to critical |
| Data calculated from Yaws data | | | |
| ρ_ℓ | kmol/m ³ | 66.155 | Density of liquid |
| ρ_{crit} | kmol/m ³ | 17.746 | Density at critical point |
| H_{ca} | kJ/mol | 61.99 | Enthalpy difference, ambient to critical |
| D | m ² /s | 5.516×10^{-6} | Thermal diffusivity |
| eta _{eff} | mPa·s | 19.465 | Effective viscosity, Eq. (34) in West (1998) |

REFERENCES

- Blander, M. and Katz, J. L. 1975. "Bubble Nucleation in Liquids," *AIChE Journal* **21**, 5, 833–848, September.
- Briggs, L. J. 1953. "The Limiting Negative Pressure of Mercury in Pyrex Glass," *Jnl. Appl. Phys.* **24**, 1, 488–490, April.
- Chute 1896. "Physical Laboratory Manual," Section 67, D. C. Heath & Co., 1896.
- Fu, Chia Y. 1999. Private communication with author.
- Glaser, D. A. 1994. "Invention of the Bubble Chamber and Subsequent Events," *Nucl. Phys. B (Proc. Suppl.)* **36**, 3–18.
- Glaser, D. A. and Rahm, D. C. 1955. "Characteristics of Bubble Chambers," *Physical Review* **97**, 2, 474–479.
- Hahn, B. 1961. "The Fracture of Liquids under Stress Due to Ionizing Particles," *Nuovo Cimento* **22**, 650–653.
- Hahn, B. and Peacock, R. N. 1963. "Ultrasonic Cavitation Induced by Neutrons," *Nuovo Cimento* **28**, 2, 334–340, April 16.
- Hughes, A. L. 1960. "An Exploration of the Possibility of Employing Ultrasonic Radiation to Sensitize a Bubble Chamber," in *Proceedings of the International Conference on Instrumentation for High Energy Physics*, II b.1, E. O. Lawrence Radiation Laboratory, Berkeley, California. September 12–14.
- Lieberman, D. 1959. "Radiation Induced Cavitation," *Phys. Fluids* **2**, 4, 466–468.
- Moraga, F. and Taleyarkhan, R. P. 1999. "Static and Transient Cavitation Threshold Measurements for Mercury," in *Proceedings of the 3rd International Topical Meeting on Accelerator Applications (AccApp '99)*, Long Beach, California, pp. 301–307, November.
- Pless, I. A. and Plano, R. J. 1956. "Negative Pressure Isopentane Bubble Chamber," *Rev. Sci. Instr.* **27**, 11, 935–937, November.
- Riepe, G. and Hahn, B. 1961. "Untersuchungen zum Mechanismus der Blasenbildung in Freon-12 und Propan durch Rückstoskerne einiger α -Strahler," *Helv. Phys. Acta* **34**, 8, 865–892.
- Seitz, F. 1957. "On the Theory of the Bubble Chamber," *Phys. Fluids* **1**, 1, 2–13.
- Taleyarkhan, R. P. and Kim, S. H. 1998. "Comparison of Predictions Against Thermal Shock Data in Mercury Targets," in *Proceedings of the 2nd International Topical Meeting on Accelerator Applications (AccApp '98)*, Gatlinburg, Tennessee, September.
- Taleyarkhan, R. P., Moraga, F., and West, C. D. 1998. "Experimental Determination of Cavitation Thresholds in Water and Mercury," in *Proceedings of the 2nd International Topical Meeting on Accelerator Applications (AccApp '98)*, Gatlinburg, Tennessee, pp. 650–657, September.
- West, C. D. 1967. *Cavitation Nucleation by Energetic Particles*, AERE-R5486, June.
- West, C. D. 1998. *Cavitation Bubble Nucleation by Energetic Particles*, ORNL/TM-13683, December.
- Yaws, C. L. 1996. "Floppy Disk Databases of Thermodynamic and Transport Properties," TREI, 685 Birchwood, Port Neches, Texas 77651.

INTERNAL DISTRIBUTION

- | | |
|----------------------|-------------------------------------|
| 1. Chia Y. Fu | 6-8. C. D. West |
| 2. T. A. Gabriel | 9. D. M. Williams |
| 3. J. R. Haines | 10-11. Central Research Library |
| 4. J. B. Roberto | 12. ORNL Laboratory Records—RC |
| 5. R. P. Taleyarkhan | 13-14. ORNL Laboratory Records—OSTI |

EXTERNAL DISTRIBUTION

15. Prof. R. E. Apfel, Yale University, 9 Hillhouse Avenue, New Haven, CT 06520-8286
16. Dr. G. Bauer, Paul Scherrer Institute, CH5232, Villigen, Switzerland
17. Prof. F. d'Errico, Yale University School of Medicine, Department of Therapeutic Radiology, Division of Radiological Physics, 333 Cedar St., HRT-219, New Haven, CT 06510
18. Herr Dr. Georg Riepe, Im Schmidtenloch 59, D-53894 Mechernich, Germany
19. Dr. Carl L. Yaws, TREI, 685 Birchwood, Port Neches, TX 77651
20. D. K. Wilfert, U.S. Department of Energy, Bldg. 701SCA, MS-6477, P.O. Box 2001-LM-14, Oak Ridge, TN 37831-6477